

Generalizing Adam To Manifolds For Efficiently Training Transformers

Benedikt Brantner

(benedikt.brantner@ipp.mpg.de) 

Max-Planck-Institut für Plasmaphysik

Boltzmannstraße 2, 85748 Garching, Deutschland

and

Technische Universität München, Zentrum Mathematik

Boltzmannstraße 3, 85748 Garching, Deutschland

October 1, 2024

Abstract

One of the primary reasons behind the success of neural networks has been the emergence of an array of new, highly-successful optimizers, perhaps most importantly the Adam optimizer. It is widely used for training neural networks, yet notoriously hard to interpret. Lacking a clear physical intuition, Adam is difficult to generalize to manifolds. Some attempts have been made to directly apply parts of the Adam algorithm to manifolds or to find an underlying structure, but a full generalization has remained elusive.

In this work a new approach is presented that leverages the special structure of the manifolds which are relevant for optimization of neural networks, such as the Stiefel manifold, the symplectic Stiefel manifold, the Grassmann manifold and the symplectic Grassmann manifold: all of these are homogeneous spaces and as such admit a global tangent space representation.

This global tangent space representation is used to perform all of the steps in the Adam optimizer and we are able to fully generalize the optimizer to manifolds without a projection step. The resulting algorithm is then applied to train a transformer for which orthogonality constraints are enforced up to machine precision and we observe significant speed-ups in the training process.

Keywords: Adam optimizer, neural network training, manifold optimization, Stiefel manifold, homogeneous spaces, deep learning, deep neural networks, transformer, orthogonality constraints, vanishing gradients, parallel programming

MSC 2020: 53Z50, 53C30, 68T07, 68W10, 90C26

Contents

1	Introduction and Related Work	3
2	The new Optimizer Framework	5
3	Homogeneous Spaces and a Global Tangent Space Representation	10
4	Numerical Example: the Transformer	13
5	Conclusion and Outlook	16
	References	17
	Appendices	21
A	Induced Isomorphism	21
B	Computing the Lift $Y \mapsto \lambda(Y)$	21
C	Computing Exponentials	21
D	The Cayley Retraction	22
E	Parallel Transport	23
F	The Softmax Activation Function and the Classification Layer	25
G	Computing Correlations in the Multihead-Attention Layer	25

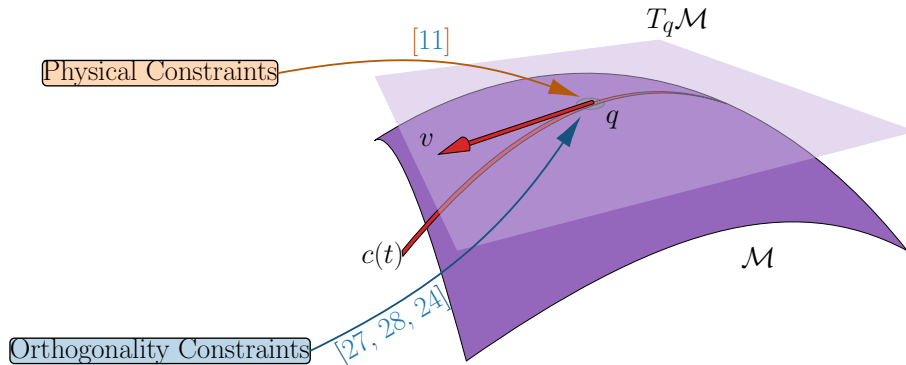


Figure 1: The motivation for manifold optimization comes from different angles: (i) for many applications manifold optimization can bring huge improvements in training the network through e.g. automatically enforced orthogonality constraints [27, 28, 24]; (ii) for applications in physics certain network architectures, like the ones presented in [11], require manifold optimization. In this work we focus on point (i) to demonstrate the efficacy of the new optimizers.

1 Introduction and Related Work

The enormous success of neural networks in recent years has in large part been driven by the development of new and successful optimizers, most importantly Adam [22]. Even though the Adam algorithm is nowadays used to train a wide variety of neural networks, its theoretical properties remain largely obscure [25].

Besides new optimizers, another source of advancement in neural network research has been the inclusion of specific problem-dependent penalization terms into the loss functional, i.e. problem-specific terms are added to the loss function as

$$\tilde{J}(\text{weights}; \text{data}) = J(\text{weights}; \text{data}) + \mu\Omega(\text{weights}), \quad (1)$$

where Ω is called the “regularizer” [20]. Two of the most important of these regularization terms are (i) orthogonality constraints (see [41] for an application to transformer neural networks and [3] for an application to convolutional neural networks) and (ii) properties relating to a physical system, yielding *physics-informed neural networks* (PINNs, [32]); so these terms are accounted for through the additional loss Ω . Despite successful application in many different settings, an inherent problem is that these regularizers do not provide theoretical guarantees on the preservation of relevant properties and that they rely on extensive hyperparameter tuning. Regularization terms often make training neural networks difficult, cumbersome and “unpredictable” [23].

What would make these extra terms in the loss functional and the associated hyperparameters redundant would be optimization on spaces that satisfy the associated constraints automatically [4, 28, 24, 29, 27]. Such spaces are in many cases *homogeneous spaces* (see [31, Chapter 11] and [17, Chapter 17]), a special class of manifolds. Homogeneous spaces that are important for neural networks include the Stiefel manifold [28, 24], the Grassmann manifold (see the documentation of [10]) and the “space of positions and orientations” [38]. Regarding point (i), it will be shown in Section 4 that optimization on spaces that preserve orthonormality can enable training in some cases in which it otherwise would not be possible; in other cases it can speed up training immensely [24]. For point (ii), the case when the network has to be imbued with physical properties, optimizing on manifolds can be inevitable [11]. We sketch these two different motivations in Figure 1.

In order to fully benefit from introducing manifolds into neural networks, existing powerful optimizers should be extended to this setting, but the obscure nature of the Adam algorithm has meant that its properties have to be severely restricted before this extension can be made.¹

A first, partly successful, attempt at generalizing Adam is shown in [28], but does not capture the structure of the second moments (see Equation (11)). The approach presented in [24] is more involved and the most-closely related one to this work. The authors formulate the optimization problem as an unconstrained variational problem with Lagrangian on the Stiefel manifold² $\mathcal{M} := \{Y \in \mathbb{R}^{N \times n} : Y^T Y = \mathbb{I}_n\}$:

$$\mathfrak{L}(Y, \dot{Y}, \Lambda, t) = r(t) \left[\frac{1}{2} \text{Tr} \left(\dot{Y}^T (I - a Y Y^T) \dot{Y} \right) - L(Y) \right] - \frac{1}{2} \text{Tr} \left(\bar{A}^T (Y^T Y - I) \right), \quad (2)$$

where a is a parameter that defines a one parameter *family of Riemannian metrics* on the Stiefel manifold \mathcal{M} , i.e. $g_a : T_Y \mathcal{M} \times T_Y \mathcal{M} \rightarrow \mathbb{R}^+$, $(V_1, V_2) \mapsto \frac{1}{2} \text{Tr}(V_1^T (I - a Y Y^T) V_2)$, and L is the loss function to be minimized. In this description Y , which are elements of \mathcal{M} , are parameters of the neural network and $\bar{A} \in \mathbb{R}^{n \times n}$ is a Lagrange multiplier that enforces the constraint that the neural network weights have to be elements of the Stiefel manifold.

The authors obtain equations of motion through the variational principle and these are then discretized by a clever splitting scheme to obtain the final optimizer, which is used for training the neural network. Stochastic gradient descent (SGD) with momentum is in this case just the solution of the variational problem, which the authors call ‘‘Momentum SGD’’. In order to obtain a version of Adam, the authors apply a modification to this algorithm to include second moments. This step, however, involves a projection step and thus does not generalize Adam completely. As for applications, the authors’ main practical objective is, as it is in this paper, to train a transformer [39].

The approach presented in [27] is also related to this work; in there the authors design an optimization scheme for which a single update³ is

$$e^A \leftarrow \exp(A - \eta \nabla(L \circ \exp)(A)). \quad (3)$$

With this approach the Adam optimizer can be generalized to Lie groups, but not to homogeneous spaces. Acknowledging this the authors conclude [27] by saying: ‘‘Additionally, it could be of interest to see how orthogonal constraints help with learning in deep feed forward networks. In order to make this last point formal, one would have to generalize the results presented here to homogeneous Riemannian manifolds, like the Stiefel manifold.’’ In this work we show how to perform this ‘‘generalization’’ and therefore extend the *stat-of-the-art* of optimization on homogeneous spaces for neural networks by introducing an optimization framework from which standard optimizers (such as Adam) can be recovered naturally - this is not possible with other manifold optimizers for neural networks such as [28, 24]. We visualize the idea behind our approach in Figure 2.

The remainder of this paper is organized as follows: Section 2 presents a high-level description of our approach and discusses the associated operations in some detail. It

¹This is not true for optimizers that only contain first moments but no second moments (like the Adam optimizer). Optimizers that only contain first moments admit a variational formulation and allow for straightforward generalization to arbitrary manifolds [15, 24].

²The Stiefel manifold will be discussed in detail in Section 3.

³As was already explained in [27] the exponential map can be replaced with a *retraction* [1] (also confer Definition 4).

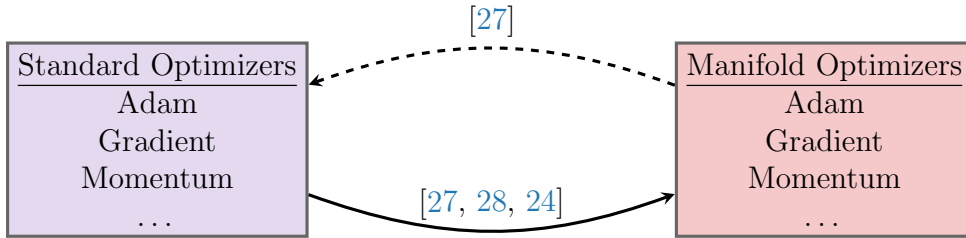


Figure 2: There exist various approaches for constructing neural network optimizers for the Stiefel manifold [28, 24], but with those approaches one cannot recover the original optimizer (left) from the manifold version (right). When dealing with Lie groups (a more restrictive class of manifolds than homogeneous spaces) the approach proposed in [27] offers a way of constructing a manifold optimizer from which the vector space one can be recovered.

is shown how Adam can be recovered as a special case of this more general framework. Section 3 gives a description of all the relevant aspects of homogeneous spaces that are needed for our framework and Section 4 shows an application of the new optimizers for training a transformer. The new optimizers are part of the `Julia` package `Geometric-MachineLearning.jl` [10].

Throughout the discussion, the Stiefel manifold will be used as an example to elucidate the more abstract and general concepts; however the mathematical constructions are very general and can, in addition to the Stiefel manifold, be applied to the Grassmann manifold [6], the symplectic versions of the two manifolds [5] as well as the “homogeneous space of positions and orientations” [38].

2 The new Optimizer Framework

In this section we introduce our new framework. Some of the terminology introduced here (like $\mathfrak{g}^{\text{hor}}$) will be explained in Section 3. Here our primary goal is to show that standard optimizers (especially the Adam optimizer) can be recovered from our new framework by making simplifications (i.e. we can realize the dashed arrow in Figure 2). This is not possible with other attempts at generalizing Adam to homogeneous spaces [24, 28]. Different from other approaches we use Operations 1 to 3 to allow for this generalization. After having introduced these operations we show how to recover the Adam optimizer from this more general framework⁴.

Modern optimization of neural networks is almost always done with some version of gradient descent that takes two inputs: a differentiated loss function $\nabla_{\mathcal{Y}} L \equiv \nabla L$, which is the output of an automatic differentiation (AD)⁵ routine, and a `cache` that stores information about previous gradient descent steps (see e.g. [20, chapter 8]).

In the framework presented here, a high-level optimization algorithm for general neural networks takes the form shown in Algorithm 1. We further visualize the new optimizer framework (along with traditional vector space optimization) in Figure 3.

For the case for which the weights lie on a vector space \mathcal{V} (a special case of a homo-

⁴We only treat the Adam optimizer, the *gradient optimizer* and the *momentum optimizer* in this work. The framework is however also readily generalizable to e.g. the BFGS optimizer [37, Chapter 6.1].

⁵AD underpins the training of practically every deep neural network, but its discussion would be beyond the scope of this paper; [21, 9] offer a rigorous and detailed discussion of AD. For the purposes of this paper an AD routine simply takes a loss function L as input and returns its (Euclidean) gradient with respect to the weights of the neural network $\nabla_{\mathcal{Y}} L \equiv \nabla L$.

Algorithm 1 High-level optimization algorithm for neural networks

Require: time t , weights $Y^{(t)}$, `cache`, differential ∇L , \mathcal{O} -parameters Ξ , section $\Lambda^{(t)}$;
 $t \leftarrow t + 1$
 $\Delta^{(t)} \leftarrow \text{rgrad}(\nabla L)$ ▷ compute the Riemannian gradient.
 $\mathcal{B}^{(t)} \leftarrow \text{global_rep}(Y^{(t)}, \Delta^{(t)})$ ▷ compute the lifted version of $Y^{(t)}$.
`cache` $\leftarrow \text{update}(\text{cache}, \mathcal{B}^{(t)}, t, \Xi)$ ▷ update cache based on $\mathcal{B}^{(t)}$.
 $W^{(t)} \leftarrow \text{velocity}(\text{cache}, \Xi)$ ▷ compute final velocity.
 $\Lambda^{(t+1)} \leftarrow \text{update_section}(\Lambda^{(t)}, \mathcal{B}^{(t)})$
 $Y^{(t+1)} \leftarrow \text{apply_section}(\Lambda^{(t)}, E)$ ▷ multiplication with the *distinct element* E .

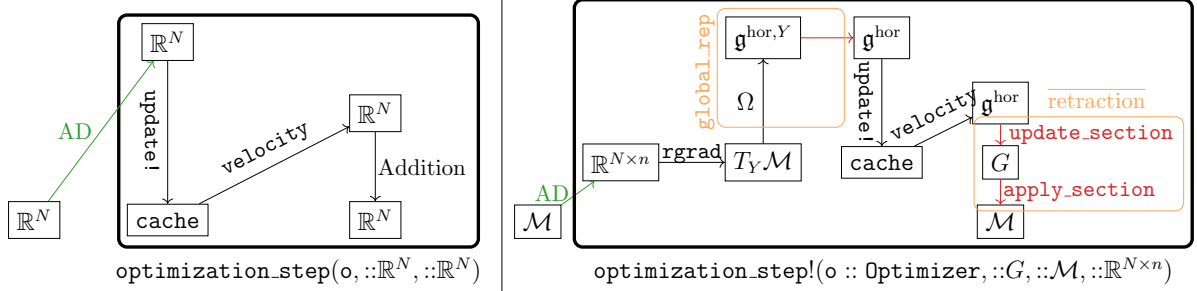


Figure 3: Comparison between regular Adam and Adam adapted to manifolds. A red color indicates that the operation requires the *global section* $\Lambda^{(t)}$. An orange color indicates that the operation is the result of grouping two individual operations together. Crucially, with the framework presented in this work we can recover the optimizer shown on the left from the one on the right if the manifold \mathcal{M} is a vector space.

geneous space), the functions `rgrad`, `global_rep` and `retraction`⁶ are greatly simplified. Specifically:

- `rgrad` and `global_rep` are identity mappings.
- `retraction` is standard “addition”. Note that in Figure 3 we split `retraction` up into two mappings: `update_section` and `apply_section`. When we deal with a vector space \mathcal{V} , `update_section` is addition and `apply_section` is the identity.
- the *distinct element* $E \in \mathcal{M}$ is the zero element $\mathbb{O} \in \mathcal{V}$. The special role of this distinct element is explained in Section 3.

The other mappings, i.e. `update!` and `velocity`, as well as the structure of the `cache` and the parameters of the optimizer (called \mathcal{O} -parameters in Algorithm 1), are however equivalent in both cases (in Section 4 we explicitly list the \mathcal{O} -parameters we use). A comparison between those two scenarios is shown in Figure 3. We therefore call the `update!` method, the `velocity` method and the `cache` together an *optimizer method*.

Definition 1 (optimizer method). *The `update!` method, `velocity` method and the `cache` together constitute an **optimizer method**. The `update!` method updates the `cache` and the `velocity` method computes a final velocity. This is then used to update the neural network parameters. The optimizer method is the same irrespective of whether we deal with vector spaces or homogeneous spaces.*

⁶As is shown in Figure 3 `retraction` is the composition of `update_section` and `apply_section`. We call `retraction` an *extended retraction* (see Operation 3).

Algorithm 1 comprises all common first-order optimization algorithms such as (stochastic) gradient descent (with and without momentum), Adam and BFGS. The mappings `rgrad`, `global_rep`, `update_section` and `apply_section`, which are needed in addition to the usual steps performed by an optimizer for vector spaces, are now discussed in detail.

Operation 1 (`rgrad`). *This function computes the Riemannian gradient of a loss function L on a Riemannian matrix manifold $\mathcal{M} \subset \mathbb{R}^{N \times n}$ based on its Euclidean gradient $\nabla L \in \mathbb{R}^{N \times n}$.*

For matrix manifolds with Riemannian metric g , `rgrad` can always be found since the Euclidean gradient corresponds to an element of the cotangent space $T_Y^* \mathcal{M}$ and every element of $T_Y^* \mathcal{M}$ can be converted to an element of $T_Y \mathcal{M}$ with a Riemannian metric (see [8, Chapter 5]):

$$\langle dL, V \rangle \equiv \text{Tr}((\nabla_Y L)^T V) = g_Y(\text{rgrad}(Y, \nabla_Y L), V), \quad \forall V \in T_Y \mathcal{M}. \quad (4)$$

For the Stiefel manifold (see Section 3) the canonical metric and the associated gradient are:

$$g_Y(V_1, V_2) = \text{Tr} \left(V_1^T \left(\mathbb{I} - \frac{1}{2} Y Y^T \right) V_2 \right), \quad (5)$$

and

$$\text{grad}_Y L = \text{rgrad}(Y, \nabla L) = \nabla L - Y \nabla L^T Y. \quad (6)$$

For homogeneous spaces there is a natural way of obtaining a metric and we hence call this metric the *canonical metric*. This is discussed in Section 3. After we have applied `rgrad`, we get an element in $T_Y \mathcal{M}$. We cannot use this for updating the `cache` however, since the parametrization of this tangent vector depends on the specific tangent space $T_Y \mathcal{M}$. In order to get around this issue we need the notion of a *global tangent space representation*:

Definition 2 (Global Tangent Space Representation). *A vector space $\mathfrak{g}^{\text{hor}}$ that is isomorphic to $T_Y \mathcal{M}$ for each $Y \in \mathcal{M}$.*

Remark. *Of course every manifold has such a global tangent space representation, because $T_Y \mathcal{M} \simeq \mathbb{R}^d$ where $d = \dim \mathcal{M}$. But usually the mappings $T_Y \mathcal{M} \rightarrow \mathbb{R}^d$ are very difficult to find. What we exploit here is that for homogeneous spaces however this is relatively easy (see Definition 7).*

We for now define the global tangent space $\mathfrak{g}^{\text{hor}}$ as some vector space for which we can easily find isomorphisms $T_Y \mathcal{M} \simeq \mathfrak{g}^{\text{hor}}$ for every $Y \in \mathcal{M}$; we will give an explicit construction in Section 3. We can now describe the operation `global_rep` in Algorithm 1:

Operation 2 (`global_rep`). *A mapping from the tangent space $T_Y \mathcal{M}$, the output of `rgrad`, to a global tangent space $\mathfrak{g}^{\text{hor}}$ that is isomorphic to $T_Y \mathcal{M}$.*

So the `global_rep` realizes one direction of the isomorphism $T_Y \mathcal{M} \xrightarrow{\sim} \mathfrak{g}^{\text{hor}}$. So every element of the tangent space $T_Y \mathcal{M}$, for every $Y \in \mathcal{M}$, can be *lifted* to $\mathfrak{g}^{\text{hor}}$. For computational purposes `global_rep` is performed in two steps as indicated in Figure 3. This will be further explained in Section 3.

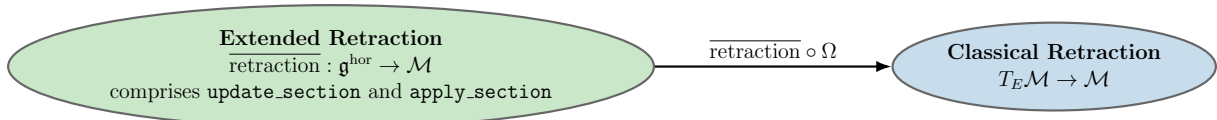


Figure 4: The *extended retraction* $\overline{\text{retraction}} : \mathfrak{g} \rightarrow \mathcal{M}$ we use in this work is different from *classical retractions* [1] but fulfills a similar role. An *extended retraction* is defined as a map from which a *classical retraction* can be recovered by composing it with another operation (see Operation 3).

Remark. If \mathcal{M} is a vector space \mathcal{V} , then $\mathcal{M} \equiv T_Y^* \mathcal{M} \equiv T_Y \mathcal{M} \equiv \mathfrak{g}^{\text{hor}} = \mathcal{V}$ and no global tangent space representation is necessary.

In order to define the operation `retraction` in Algorithm 1, we first need the notion of a *geodesic*.

Definition 3. A *geodesic* is the solution of the geodesic differential equation. It is the curve that minimizes the following functional:

$$L(\gamma) = \int_0^1 \sqrt{g_{\gamma(t)}(\dot{\gamma}(t), \dot{\gamma}(t))}. \quad (7)$$

Closely connected to the notion of a geodesic is that of the *geodesic spray*. The *geodesic spray* or *geodesic differential equation* (see [8, chapter 5]) is a second order ordinary differential equation on the manifold \mathcal{M} , so takes initial conditions on $T_Y \mathcal{M}$. Its solutions have the following property:

Proposition 1. Let $\bar{\gamma} : [0, T] \rightarrow T\mathcal{M}$ be a solution to the geodesic spray. It has the property that

$$\bar{\gamma}(t) = (\gamma(t), \gamma'(t)), \quad (8)$$

and γ is a geodesic.

For Riemmanian optimization problems [1, 35] this differential equation has to be solved exactly or approximately. If it is solved approximately, we refer to the method of approximating it as a *classical retraction*.

Definition 4. An approximation of the exponential map is referred to as **classical retraction** and is a map $\mathcal{R} : T\mathcal{M} \rightarrow \mathcal{M}$ that satisfies the following properties: $\mathcal{R}_Y(\mathbb{O}_Y) = Y$ and $T_{\mathbb{O}_Y} \mathcal{R}_Y = \text{id}|_{T_Y \mathcal{M}}$ where \mathbb{O}_Y is the zero element of the vector space $T_Y \mathcal{M}$ and $\text{id}|_{T_Y \mathcal{M}}$ is the identity map on $T_Y \mathcal{M}$.

Since the Stiefel manifold admits closed-form solutions of its geodesic (see Equation (17)) we can use these directly besides other approximations. Consequently we refer to the analytic solution of the geodesic spray as the *geodesic retraction*. In Section 4 we further compare it to the Cayley retraction [1, 28] (see Appendix D).

Remark. If the considered manifold is a vector space \mathcal{V} with the canonical metric, the geodesic is simply a straight line: $\gamma(t) = Y + tW \in \mathcal{V}$ for $Y, W \in \mathcal{V}$; i.e. the retraction is simple addition (also confer Figure 3).

For computational purposes the operation $\overline{\text{retraction}}$ shown in Figure 3 is different from Definition 4, but fulfills the same purpose. It is defined in Operation 3. Further note that $\overline{\text{retraction}}$ is, analogously to `global_rep`, split into two parts: `update_section` and `apply_section` (see Algorithm 1). We call `retraction` an *extended retraction*. We illustrate

the difference between classical retraction and the extended retraction introduced here in Figure 4.

We also note that for a geometrical sound optimization scheme the cache needs to be *parallel transported along the optimization trajectory* [1, 33]. In Appendix E we show that our algorithm performs parallel transport for the cache in the right way.

Recovering the Adam Optimizer

One can recover the *Adam optimizer* from Algorithm 1 by making the following identifications:

1. The **cache** in Adam consists of two parameters \mathcal{B}_1 and \mathcal{B}_2 for every weight, both of which are elements of $\mathfrak{g}^{\text{hor}}$. They are referred to as the *first* and *second moment*.
2. The **cache** = $(\mathcal{B}_1^{\text{cache}}, \mathcal{B}_2^{\text{cache}})$ is updated in the following way:

$$\mathcal{B}_1^{\text{cache}} \leftarrow \frac{\beta_1 - \beta_1^t}{1 - \beta_1^t} \mathcal{B}_1^{\text{cache}} + \frac{1 - \beta_1}{1 - \beta_1^t} \mathcal{B}_t, \quad \mathcal{B}_2^{\text{cache}} \leftarrow \frac{\beta_2 - \beta_2^t}{1 - \beta_2^t} \mathcal{B}_2^{\text{cache}} + \frac{1 - \beta_2}{1 - \beta_2^t} \mathcal{B}_t \odot \mathcal{B}_t, \quad (9)$$

where \odot is the element-wise Hadamard product, i.e. $(v \odot w)_i := v_i w_i$.

3. For the final velocity:

$$W_t \leftarrow \text{velocity}(\text{cache}, \Xi) = -\eta \mathcal{B}_1^{\text{cache}} / \sqrt{\mathcal{B}_2^{\text{cache}} + \delta}, \quad (10)$$

where the division $/$ and the addition with the scalar δ are done element-wise.

The \mathcal{O} -parameters (see Algorithm 1) for Adam are $\Xi = (\eta, \beta_1, \beta_2, \delta)$. The Adam **cache** and the Adam operations in equations Equations (9) and (10) are identical in the vector space and in the manifold case.

Two related approaches to what is presented here are [28], [24] and [27]. In [28] the authors approximate $\mathcal{B}_2^{\text{cache}}$ with a scalar quantity, i.e.

$$\mathcal{B}_2^{\text{cache}} \leftarrow \frac{\beta_2 - \beta_2^t}{1 - \beta_2^t} \mathcal{B}_2^{\text{cache}} + \frac{1 - \beta_2}{1 - \beta_2^t} \|\mathcal{B}_t\|^2, \quad (11)$$

which leads to speed ups in some cases, but ignores the structure of the second moments.

For the case $N = n$, the versions of Adam presented in [24] and [27] are very similar to our approach. In this case the global tangent space representation is the collection of skew-symmetric matrices⁷ $\mathfrak{g}^{\text{hor}} = \mathfrak{g} = \{\mathcal{B} \in \mathbb{R}^{N \times N} : \mathcal{B}^T + \mathcal{B} = 0\}$. In this case no lift has to be performed. But if $N \neq n$, then [24] need a projection, which our algorithm does not need and the approach shown in [27] is not able to deal with the case $N \neq n$; in other words it can only be applied to Lie groups and not to homogeneous spaces.

In Section 4 we compare Adam to two other optimizers: (i) the *gradient optimizer* and (ii) the *momentum optimizer*. Both can be derived from the general framework presented in Algorithm 1. For these two optimizers:

- (i) **cache** is empty; the final velocity W_t in Algorithm 1 is set to \mathcal{B}_t and $\Xi = (\eta)$.

⁷The skew-symmetric matrices constitute a Lie algebra (see Section 3).

- (ii) **cache** stores velocity information, i.e. consists of first moments $\mathcal{B}^{\text{cache}}$. This is updated with

$$\mathcal{B}^{\text{cache}} \leftarrow \alpha \mathcal{B}^{\text{cache}} + \mathcal{B}_t. \quad (12)$$

The velocity is then computed with $W_t \leftarrow \text{velocity}(\text{cache}, \Xi) := -\eta \mathcal{B}^{\text{cache}}$, where $\Xi = (\eta, \alpha)$.

3 Homogeneous Spaces and a Global Tangent Space Representation

In this section we discuss some aspects of homogeneous spaces that are relevant for our algorithm. More extensive treatments can be found in [31, Chapter 11] and [17, Chapter 17]. The Stiefel manifold is used as a concrete example to make abstract constructions more clear, but what is presented here applies to all homogeneous spaces such as the Grassmann manifold [6] and the “homogeneous space of positions and orientations” [38].

Definition 5. A *homogeneous space* is a manifold \mathcal{M} on which a Lie group G acts transitively, i.e. the group action $G \times \mathcal{M} \rightarrow \mathcal{M}$ is such that $\forall Y_1, Y_2 \in \mathcal{M} \exists \Lambda \in G$ s.t. $l_\Lambda Y_1 \equiv \Lambda Y_1 = Y_2$ (here l_Λ denotes the left action of an element Λ of G onto \mathcal{M}).

In the following we will associate a distinct element⁸ $E_{\mathcal{M}} \equiv E$ with every homogeneous space \mathcal{M} . Because G acts transitively on \mathcal{M} , every element of \mathcal{M} can then be represented with an element of G acting on E . As an example, consider the orthogonal group $O(N) := \{\lambda \in \mathbb{R}^{N \times N} : \lambda^T \lambda = \mathbb{I}_N\}$ and the Stiefel manifold $\mathcal{M}_{\text{Stiefel}} \equiv St(n, N) := \{Y \in \mathbb{R}^{N \times n} : Y^T Y = \mathbb{I}_n\}$. An element of $O(N)$ is a collection of N orthonormal vectors in \mathbb{R}^N and an element of $\mathcal{M}_{\text{Stiefel}}$ is a collection of n orthonormal vectors in \mathbb{R}^N where $n < N$. As distinct element for $\mathcal{M}_{\text{Stiefel}}$ we pick:

$$E = \begin{bmatrix} 1 & 0 & \dots & 0 \\ 0 & 1 & \dots & 0 \\ & \dots & \dots & \\ 0 & 0 & \dots & 1 \\ 0 & 0 & \dots & 0 \\ & \dots & \dots & \\ 0 & 0 & \dots & 0 \end{bmatrix} = \begin{bmatrix} \mathbb{I}_n \\ \mathbb{O} \end{bmatrix}, \text{ where } \mathbb{O} \in \mathbb{R}^{(N-n) \times n}. \quad (13)$$

If we now apply an element $[y_1, \dots, y_n, y_{n+1}, \dots, y_N] = \Lambda \in G$ from the left onto E , the resulting matrix consists of the first n columns of Λ : $\Lambda E = Y = [y_1, \dots, y_n]$. So multiplication with E from the right maps G to \mathcal{M} . With this we can define the notion of a *section*:

Definition 6. A *section* is a mapping $\lambda : \mathcal{M} \rightarrow G$ s.t. $\lambda(Y)E = Y$.

Sections are necessary for the computation of `global_rep` (see Operation 2). We now give a concrete example of a section: Consider the element $Y = [y_1, y_2, \dots, y_n] \in \mathcal{M}$. We want to map it to its associated Lie group $G = O(N)$. In order to do so we have to find $(N - n)$ orthonormal vectors that are also orthonormal to Y ; i.e. we have to find $Q = [q_1, \dots, q_{N-n}]$ such that $Y^T Q = \mathbb{O}_n$ and $Q^T Q = \mathbb{I}_n$. In the implementation this is

Algorithm 2 Computation of the lift $Y \mapsto \lambda(Y) \in G$ with a QR decomposition.

$A \leftarrow \mathcal{P}(\mathbb{R}^{N \times (N-n)}),$	\triangleright sample A from a given distribution.
$A \leftarrow A - YY^T A,$	\triangleright remove the part of A that is spanned by the columns of Y .
$Q, R \leftarrow \mathbf{qr}(A),$	\triangleright apply a QR decomposition.
$\lambda(Y) \leftarrow [Y, Q[1 : N, 1 : (N-n)]]$.	\triangleright output Y and the first $(N-n)$ columns of Q .

done using a QR decomposition (Householder reflections). Details of this are shown in Algorithm 2 and further discussed in Appendix B.

Remark. *We only have to perform this operation once when we initialize the optimizer. For all successive steps we parallel transport (see Appendix E) the section $\Lambda^{(t)}$ with `update_section` (see Algorithm 1 and Figure 3).*

We now proceed with introducing the remaining necessary components that are needed to introduce the global tangent space representation for homogeneous spaces. In the following we assume that the Lie group G is equipped with a Riemannian metric⁹ g .

First note that $T_Y \mathcal{M} \equiv \mathfrak{g} \cdot Y$, i.e. the tangent space at Y can be represented by the application of the Lie algebra of G to the element Y . The kernel of this map $\mathfrak{g}^{\text{ver}, Y} := \ker(\mathfrak{g} \rightarrow T_Y \mathcal{M})$ is called the *vertical component* of the Lie algebra at Y . Its complement (with respect to the Riemannian metric g on G) in \mathfrak{g} is called the *horizontal component* of \mathfrak{g} at Y and denoted by $\mathfrak{g}^{\text{hor}, Y}$; this therefore establishes an isomorphism $\mathfrak{g}^{\text{hor}, Y} \simeq T_Y \mathcal{M}$ and the mapping $\Omega : T_Y \mathcal{M} \rightarrow \mathfrak{g}^{\text{hor}, Y}$ can be found explicitly. For the Stiefel manifold this mapping is (in Appendix A we show that Ω is indeed an isomorphism):

$$\Omega(\text{grad}_Y L) = \left(\mathbb{I} - \frac{1}{2} Y Y^T \right) (\text{grad}_Y L) Y^T - Y (\text{grad}_Y L)^T \left(\mathbb{I} - \frac{1}{2} Y Y^T \right). \quad (14)$$

Also confer Figure 3 to see where this mapping appears in the algorithm. The mapping Ω naturally induces a metric on the Stiefel manifold: two vectors of $T_Y \mathcal{M}$ can be mapped to $\mathfrak{g}^{\text{hor}, Y} \subset \mathfrak{g}$ and the scalar product can be computed in the Lie algebra. If $G = O(n)$ is equipped with the canonical metric one obtains the canonical metric for the Stiefel manifold, presented in equation Equation (5). We can now define what we mean by *global tangent space representation for a homogeneous space*:

Definition 7. *To each homogeneous space we can associate a **global tangent space representation** $\mathfrak{g}^{\text{hor}, E}$ where we have identified a distinct element $E \in \mathcal{M}$. It is the horizontal component of the Lie algebra at the distinct element E . We typically simply call this $\mathfrak{g}^{\text{hor}}$.*

Mapping the output of `rgrad` (Operation 1), which is an element of $T_Y \mathcal{M}$, to the global tangent space representation $\mathfrak{g}^{\text{hor}}$ requires another mapping besides Ω ; one from $\mathfrak{g}^{\text{hor}, Y}$ to $\mathfrak{g}^{\text{hor}} \equiv \mathfrak{g}^{\text{hor}, E}$. This is the second operation that is part of `global_rep`, i.e. Operation 2, in Figure 3.

We obtain this second mapping by first computing¹⁰ or updating¹¹ a *section* of Y (see

⁸We already used the distinct element E in Algorithm 1. In the case when the homogeneous space is a vector space \mathcal{V} then the group action is addition and the distinct element is the zero element: $E = \mathbb{0} \in \mathcal{V}$.

⁹As a metric g on $G = O(N)$ we take the canonical one, i.e. $g : (V_1, V_2) \mapsto \frac{1}{2} \text{Tr}(V_1, V_2)$.

¹⁰Computing a section is only done when initializing the optimizer. For this we use Algorithm 2.

¹¹For updating the section (i.e. for successive steps after the optimizer has been initialized) we use parallel transport (see Appendix E).

Definition 6) and then performing:

$$\Omega(\text{grad}(Y, \nabla L)) \mapsto \lambda(Y)^{-1} \Omega(\text{grad}(Y, \nabla L)) \lambda(Y). \quad (15)$$

The following theorem shows that equation Equation (15) establishes an isomorphism:

Theorem 1. *The map $\mathfrak{g}^{\text{hor}, Y} \rightarrow \mathfrak{g}^{\text{hor}}$, $Z \mapsto \Lambda^{-1} Z \Lambda$ for any $\Lambda \in G$ such that $\Lambda E = Y$ is an isomorphism.*

Proof. The considered map is clearly invertible. For the remainder of the proof we have to show that $\Lambda^{-1} Z \Lambda$ is an element of $\mathfrak{g}^{\text{hor}}$ and that for every element $B \in \mathfrak{g}^{\text{hor}}$ there exists $Z_B \in \mathfrak{g}^{\text{hor}, Y}$ such that $\Lambda^{-1} Z_B \Lambda = B$.

For the first part, assume $\Lambda^{-1} Z \Lambda \notin \mathfrak{g}^{\text{hor}}$. This implies that there exists a decomposition $\Lambda^{-1} Z \Lambda = V_Z + H_Z$ with $V_Z \neq 0$ being the vertical part, i.e. $V_Z E = 0$. But then $Z = \Lambda V_Z \Lambda^{-1} + \Lambda H_Z \Lambda^{-1}$ with $0 \neq \Lambda V_Z \Lambda^{-1} \in \mathfrak{g}^{\text{ver}, Y}$. A contradiction.

For the second part, consider $B \in \mathfrak{g}^{\text{hor}}$. By a similar argument as above we can show that $\Lambda B \Lambda^{-1} \in \mathfrak{g}^{\text{hor}, Y}$. This element fulfills our requirements. \square

We further note that the particular space $\mathfrak{g}^{\text{hor}} \equiv \mathfrak{g}^{\text{hor}, E}$, the horizontal subspace of \mathfrak{g} at E , allows for an especially sparse and convenient representation. For the Stiefel manifold:

$$\mathfrak{g}^{\text{hor}} = \left\{ \left(\underbrace{\begin{bmatrix} A \\ B \end{bmatrix}}_n \underbrace{\begin{bmatrix} -B^T \\ 0 \end{bmatrix}}_{N-n} \right) : A \in \mathbb{R}^{n \times n} \text{ skew-sym, } B \in \mathbb{R}^{N \times (N-n)} \text{ arbitrary} \right\}. \quad (16)$$

For fully implementing Algorithm 1, we still have to compute **retraction** (see Operation 3). This equates to finding a geodesic (see Definition 3) or an approximation thereof (see Definition 4). To do so we utilize the following theorem:

Theorem 2. *Let Δ be an element of the tangent space $T_Y \mathcal{M}$ of a Riemannian homogeneous space \mathcal{M} with Lie group G and right-invariant metric g . Then the associated geodesics are $\gamma_{\mathcal{M}}(t; \Delta) = \gamma_G(t; \Omega(\Delta)) Y$, where γ_G denotes the geodesic on G .*

Proof. See [31, corollary 7.46]. \square

For $G = O(n)$ the geodesic map $\mathfrak{g} \rightarrow G$ is just the matrix exponential map [1]. This means that the geodesic for $\Delta \in T_Y \mathcal{M}$ takes the following form:

$$\gamma_{\mathcal{M}}(t; \Delta) = \gamma_G(t; \Omega(\Delta)) Y = \exp(t \Omega(\Delta)) \lambda(Y) E = \lambda(Y) \exp(t \mathcal{B}) E, \quad (17)$$

where \mathcal{B} is the representation of $\Omega(\Delta)$ in $\mathfrak{g}^{\text{hor}}$, i.e. $\mathcal{B} = \lambda(Y)^{-1} \Omega(\Delta) \lambda(Y)$ for a global section $\lambda(Y)$. It has also been used that

$$\begin{aligned} \exp(t \Omega(\Delta)) &= \exp(t \lambda(Y) \mathcal{B} \lambda(Y)^{-1}) = \sum_{n=0}^{\infty} \frac{1}{n!} (t \lambda(Y) \mathcal{B} \lambda(Y)^{-1})^n \\ &= \lambda(Y) \left(\sum_{n=0}^{\infty} \frac{1}{n!} (t \mathcal{B})^n \right) \lambda(Y)^{-1}. \end{aligned} \quad (18)$$

Because of the specific structure of \mathcal{B} (see equation Equation (16)) the computation of the exponential is very cheap (see [5, 18, 16, 12]). This is further discussed in Appendix C.

We now finally give the definition of retraction from Figure 3:

Operation 3 ($\overline{\text{retraction}}$). We call a map from the global tangent space to the manifold $\overline{\text{retraction}} : \mathfrak{g}^{\text{hor}} \rightarrow \mathcal{M}$ an **extended retraction** if $\overline{\text{retraction}} \circ \Omega : T_E \mathcal{M} \rightarrow \mathcal{M}$ is a classical retraction according to Definition 4 with Ω being the unique identification $T_E \mathcal{M} \rightarrow \mathfrak{g}^{\text{hor}}$.

Equation (17) is why the actual computation of the geodesic is split up into two parts, called `update_section` and `apply_section` in Figure 3. The first of these computes $\Lambda^{(t)} \exp(\mathcal{B}^{(t)})$ and the second is the right multiplication by E . If we use a retraction instead of the exponential map (which is the equivalent to the analytic *geodesic* (see Definition 3)) we take

$$\text{update_section}(\Lambda^{(t)}, \mathcal{B}^{(t)}) = \Lambda^{(t)} \text{retraction}(\mathcal{B}^{(t)}). \quad (19)$$

In Section 4 we compare two retractions: the geodesic retraction and the Cayley retraction. In Appendices C and D we show how to utilize the sparse structure of $\mathfrak{g}^{\text{hor}}$ (see Equation (16)) to make the computation of the retraction especially efficient.

4 Numerical Example: the Transformer

The transformer architecture [39], originally conceived for natural language processing tasks, and the vision transformer [14] (used for processing image data) have largely driven advances in these fields in recent years. Part of the transformer architecture’s allure is that it is a simple and elegant construction that makes the interpretation of the neural network possible, generalizes well to diverse data sets and, perhaps most importantly, its optimization is easily parallelizable which implies good performance on GPUs.

Despite all of this, caution has to be taken when training a transformer network. The original vision transformer paper [14], for example, relies on techniques such as layer normalization [2] and extensive pre-training. Here we demonstrate that this is not necessary when optimizing on the Stiefel manifold; a similar study was performed in [24]. It has also been shown in [41] that weakly enforcing orthonormality constraints, i.e. adding terms that penalize violations of orthonormality constraints, are of advantage when dealing with transformers¹². What we demonstrate in this work are very significant performance improvements when using the new, generalized Adam optimizer; these improvements in performance were only minor in other works [28, 24].

We train the neural network on the MNIST data set [13] and the Fashion-MNIST data set [40]: for both the training data each consist of 60000 labelled (28×28) images and the test data consist of 10000 labelled (28×28) images. In order to apply the vision transformer, the data are split into 16 (7×7) image patches (similar to what was done in [14]), and these collections of 49-dimensional vectors are directly fed into the transformer. The preprocessing steps and the resulting input to the transformer (a 49×16 matrix) are shown in Figure 5. With the notation used in Section 3 we have $N = 49$ and $n = 7$. The optimizers have been implemented as part of the Julia library `GeometricMachineLearning.jl`¹³ and all the training is done on an NVIDIA Geforce RTX 4090.

The right part of Figure 5 shows the transformer architecture. Its most important part are “multihead attention modules” (introduced by [39]). Taking as input a matrix

¹²This requires an additional hyperparameter however and this can make training difficult.

¹³<https://github.com/JuliaGNI/GeometricMachineLearning.jl>. For the GPU implementation `GeometricMachineLearning.jl` uses `CUDA.jl` [7].

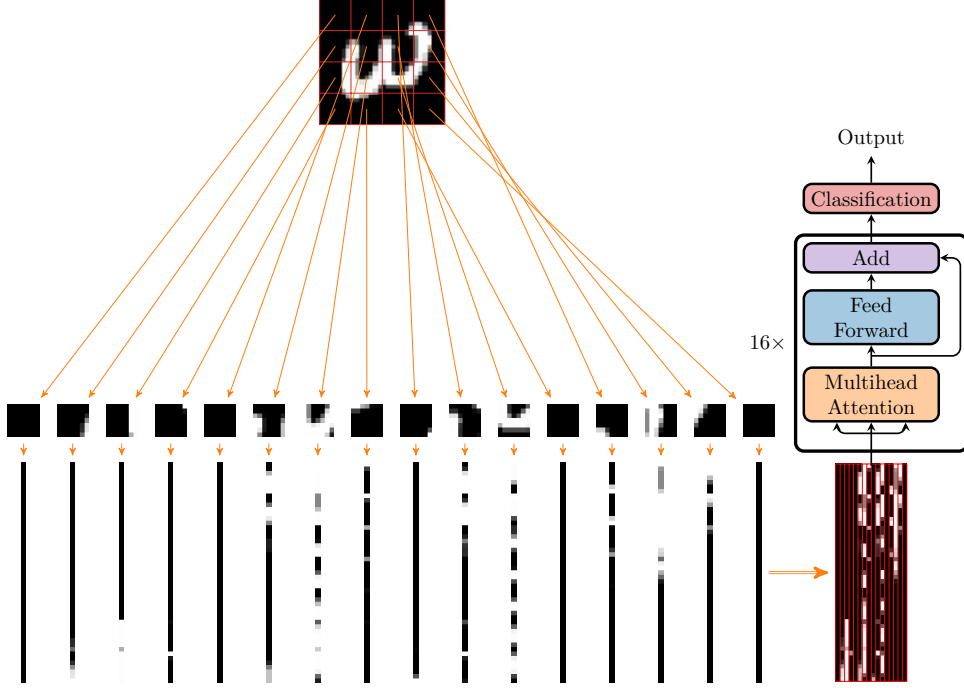


Figure 5: Preprocessing of the images is done in two steps. First the image is split into 16 patches of size 7×7 . In the second step the images are flattened and then put together again, yielding a 49×16 matrix. The output is then fed into the transformer.

$I \in \mathbb{R}^{49 \times 16}$ (the result of preprocessing an image), a single multihead attention layer performs three computations:

- (i) Computing three projections (via the matrices W_i^Q , W_i^K and W_i^V) for each index i . The index $i = 1, \dots, 7$ indicates the number of the attention head (here we have seven heads).
- (ii) Weighting the projected “values” $V_i := W_i^V I$ by the “queries” $Q_i := W_i^Q I$ and the “keys” $K_i := W_i^K I$ via an attention mechanism:

$$\hat{V}_i := \text{Attention}(Q_i, K_i, V_i) = V_i \text{softmax}(Q_i^T K_i), \quad (20)$$

where the softmax (see Appendix F) is computed column-wise.

- (iii) Rearranging the seven smaller matrices $\in \mathbb{R}^{7 \times 16}$, the seven outputs of the previous step, into a bigger matrix $\in \mathbb{R}^{49 \times 16}$ by concatenating them, i.e. the output of the multihead attention layer is $[\hat{V}_1^T \ \dots \ \hat{V}_7^T]^T$.

So in step (i) the 49-dimensional vectors of the input matrix (see Figure 5) are projected to seven-dimensional vectors with three different projection matrices to obtain “values”, “queries” and “keys”. In step (ii) correlations between the queries and keys are computed via scalar products and these are used to calculate a reweighting of the values.

In our experiments the matrices W_i^Q , W_i^K and W_i^V in the multihead-attention layers are constrained to lie on the Stiefel manifold (except for *standard Adam optimizer* which gives the blue lines in Figure 6). See Appendix G for a further theoretical motivation for this. After applying the multihead attention layer as a preprocessing step, the output is fed into a *single-layer feedforward neural network with an add connection*, i.e.

$$\text{feedforward} : x \mapsto x + \sigma(Ax + b). \quad (21)$$

For this all weights are unconstrained, i.e. $A \in \mathbb{R}^{49 \times 49}$ and $b \in \mathbb{R}^{49}$. In our neural network we use 16 such transformer layers (as indicated in Figure 5). The output of the last transformer is then finally fed into a classification layer that does:

$$\text{classification} : \mathbb{R}^{49 \times 7} \rightarrow \mathbb{R}^{10}, X \mapsto \text{softmax}(WX[1 : 49, \text{end}]). \quad (22)$$

This layer takes the last column of the output matrix, multiplies it with a learnable matrix $W \in \mathbb{R}^{10 \times 49}$ and composes it with a softmax.

For the actual *training of the transformer* we compare four different cases: (i) the transformer with all projection matrices on $\mathbb{R}^{49 \times 7}$ and trained with Adam; putting all projection matrices on the Stiefel manifold and optimizing with (ii) gradient descent (iii) gradient descent with momentum and (iv) Adam. We also call (ii) the *gradient optimizer* and (iii) the *momentum optimizer* (see Section 2).

The \mathcal{O} -parameters Ξ (see Algorithm 1) are set to the following values:

Gradient optimizer:	$\eta = 0.001.$
Momentum optimizer:	$\eta = 0.001, \quad \alpha = 0.5.$
Adam optimizer:	$\eta = 0.001, \quad \beta_1 = 0.9, \quad \beta_2 = 0.99, \quad \delta = 3 \cdot 10^{-7}.$

These particular values for the Adam optimizer are typically used as a default and usually do not need much tuning (see [20, chapter 8]). The batch size is set to 2048 and the network is trained for 500 epochs. The data as well as all network parameters are in single precision. For all experiments the regular neural network weights (i.e. the ones in the feedforward neural network and in the classification layer) are initialized with *Glorot uniform* [19]. The weights that belong to the Stiefel manifold are initialized according to Algorithm 3. The probability distributions \mathcal{P} in Algorithms 2 and 3 are chosen as products of normal distributions, called with `randn(N, n)` in many programming languages.

Algorithm 3 Initializing elements on the Stiefel manifold

$A \leftarrow \mathcal{P}(\mathbb{R}^{N \times n}),$	\triangleright sample $A \in \mathbb{R}^{N \times n}$ from a given distribution.
$Q, R \leftarrow \text{qr}(A)$	\triangleright apply a QR decomposition.
$Q[:, 1 : n]$	\triangleright output the first n columns of Q .

The blue lines in Figure 6 show the training of the transformer with Adam for which all the weights are on vector spaces $\mathbb{R}^{49 \times 7}$ (as is usually done), and the red lines show the training with Adam for the case for which the *projections* W_i^Q , W_i^K and W_i^V in the multi-head attention layer are constrained to lie on the Stiefel manifold. The gradient optimizer (in purple) and momentum optimizer (in orange) are also shown; we put the weights on the Stiefel manifold for both of these. The x -axis in Figure 6 shows the epoch and the y -axis the training loss.

For all of these computations no hyperparameter tuning has been performed. In summary the vision transformer without regularization, dropout or normalization is not able to learn much, as the error rate is stuck at around 1.34, which indicates a trivial prediction (see Appendix F).

As for the comparison of different Stiefel manifold optimizers in Figure 6 (the red, purple and orange lines), similar speed-ups are observed as for the Adam optimizer for

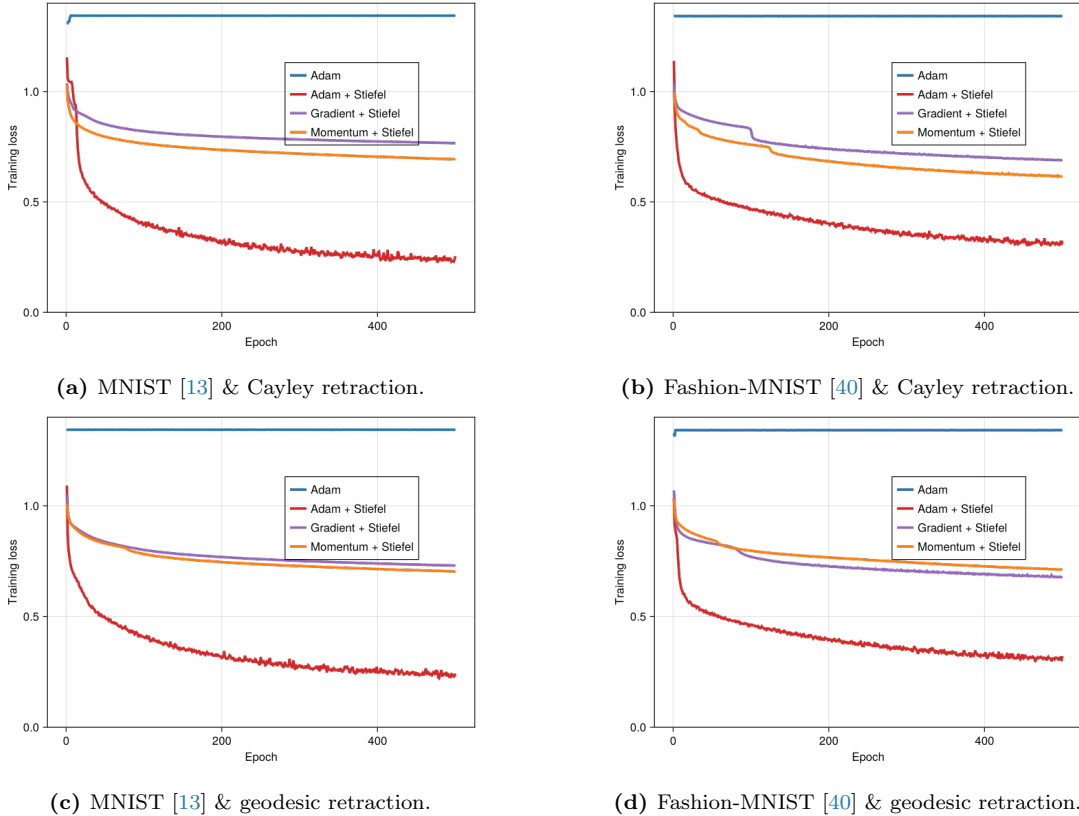


Figure 6: Training errors for the vision transformer in Figure 5. We compare different data sets and retractions here.

regular neural networks [22]. This is not the case for other manifold version of the Adam optimizer [28, 24].

We further observe some discrepancies when using different data sets (i.e. MNIST or Fashion-MNIST) and retractions (i.e. the geodesic retraction and the Cayley retraction). In all the experiments the Adam optimizer with weights on the Stiefel manifold performs best and in almost all of the experiments the momentum optimizer with weights on the Stiefel manifold performs second best. The only case where this is not true is when we train the transformer on Fashion-MNIST and use the geodesic retraction (see Figure 6(d)): here the gradient optimizer performs slightly better than the momentum optimizer.

5 Conclusion and Outlook

A generalization of Adam to homogeneous spaces (such as the Stiefel manifold) has been presented. Unlike other *start-of-the-art* manifold optimizers [28, 24] we manage to fully generalize the Adam optimizer to homogeneous spaces. The Adam optimizer for vector spaces can be recovered as a special case by setting the homogeneous space \mathcal{M} and the associated Lie group G equal to a vector space \mathcal{V} , i.e. $\mathcal{M} = G = \mathcal{V}$. This was previously only possible for optimizers on Lie groups¹⁴ [27].

It has been demonstrated that the resulting optimizers greatly simplify the training of transformer neural networks, as no special techniques like dropout, layer normalization or regularization (and the associated hyperparameter tuning) are needed to achieve conver-

¹⁴Lie groups form a more restrictive category of manifolds than homogeneous spaces.

gence. This makes the new optimizers suitable for many applications. They can facilitate training for relatively big transformers (as was shown here) and enable the incorporation of structure preservation [11].

This work also solves the challenge posed by [27] as it “generalizes [previous optimizers] to homogeneous Riemannian manifolds, like the Stiefel manifold.”

In addition, an efficient GPU implementation as part of the software package `GeometricMachineLearning.jl` [10] means training the network with manifold structure does not require much more time than training the network without manifold structure.

Future work will focus on applying the framework presented in this work to the BFGS optimizer and others [37] and an extensive comparison between the framework presented here and neural networks for which orthogonality (or similar) constraints are enforced weakly through the loss function [41].

Acknowledgements

The author would like to thank Michael Kraus and Tobias Blickhan for valuable discussions and help with the implementation.

References

- [1] P-A Absil, Robert Mahony, and Rodolphe Sepulchre. *Optimization algorithms on matrix manifolds*. Princeton University Press, Princeton, New Jersey, 2008.
- [2] Jimmy Lei Ba, Jamie Ryan Kiros, and Geoffrey E Hinton. Layer normalization. *arXiv preprint arXiv:1607.06450*, 2016.
- [3] Nitin Bansal, Xiaohan Chen, and Zhangyang Wang. Can we gain more from orthogonality regularizations in training deep networks? *Advances in Neural Information Processing Systems*, 31, 2018.
- [4] Gary Bécigneul and Octavian-Eugen Ganea. Riemannian adaptive optimization methods. *arXiv preprint arXiv:1810.00760*, 2018.
- [5] Thomas Bendokat and Ralf Zimmermann. The real symplectic stiefel and grassmann manifolds: metrics, geodesics and applications. *arXiv preprint arXiv:2108.12447*, 2021.
- [6] Thomas Bendokat, Ralf Zimmermann, and P-A Absil. A grassmann manifold handbook: Basic geometry and computational aspects. *arXiv preprint arXiv:2011.13699*, 2020.
- [7] Tim Besard, Christophe Foket, and Bjorn De Sutter. Effective extensible programming: Unleashing Julia on GPUs. *IEEE Transactions on Parallel and Distributed Systems*, 2018. ISSN 1045-9219. doi: 10.1109/TPDS.2018.2872064.
- [8] Richard L Bishop and Samuel I Goldberg. *Tensor analysis on manifolds*. Dover Publications, Mineola, New York, 1980.

- [9] Jérôme Bolte and Edouard Pauwels. A mathematical model for automatic differentiation in machine learning. *Advances in Neural Information Processing Systems*, 33: 10809–10819, 2020.
- [10] Benedikt Brantner and Michael Kraus. Geometricmachinelearning.jl: Structure-preserving neural networks. <https://github.com/JuliaGNI/GeometricMachineLearning.jl>, 2020. Accessed on September 28th 2024.
- [11] Benedikt Brantner and Michael Kraus. Symplectic autoencoders for model reduction of hamiltonian systems. *arXiv preprint arXiv:2312.10004*, 2023.
- [12] Elena Celledoni and Arieh Iserles. Approximating the exponential from a lie algebra to a lie group. *Mathematics of Computation*, 69(232):1457–1480, 2000.
- [13] Li Deng. The mnist database of handwritten digit images for machine learning research. *IEEE Signal Processing Magazine*, 29(6):141–142, 2012.
- [14] Alexey Dosovitskiy, Lucas Beyer, Alexander Kolesnikov, Dirk Weissenborn, Xiaohua Zhai, Thomas Unterthiner, Mostafa Dehghani, Matthias Minderer, Georg Heigold, Sylvain Gelly, et al. An image is worth 16x16 words: Transformers for image recognition at scale. *arXiv preprint arXiv:2010.11929*, 2020.
- [15] Valentin Duruisseaux and Melvin Leok. Accelerated optimization on riemannian manifolds via discrete constrained variational integrators. *Journal of Nonlinear Science*, 32(4):42, 2022.
- [16] Catherine Fraikin, K Hüper, and P Van Dooren. Optimization over the stiefel manifold. In *PAMM: Proceedings in Applied Mathematics and Mechanics*, volume 7, pages 1062205–1062206. Wiley Online Library, 2007.
- [17] Theodore Frankel. *The geometry of physics: an introduction*. Cambridge university press, Cambridge, UK, 2011.
- [18] Bin Gao, Nguyen Thanh Son, and Tatjana Stykel. Optimization on the symplectic stiefel manifold: Sr decomposition-based retraction and applications. *arXiv preprint arXiv:2211.09481*, 2022.
- [19] Xavier Glorot and Yoshua Bengio. Understanding the difficulty of training deep feedforward neural networks. In Yee Whye Teh and Mike Titterton, editors, *Proceedings of the Thirteenth International Conference on Artificial Intelligence and Statistics*, volume 9 of *Proceedings of Machine Learning Research*, pages 249–256, Chia Laguna Resort, Sardinia, Italy, 13–15 May 2010. PMLR. URL <https://proceedings.mlr.press/v9/glorot10a.html>.
- [20] Ian Goodfellow, Yoshua Bengio, and Aaron Courville. *Deep learning*. MIT press, Cambridge, MA, 2016.
- [21] Andreas Griewank. A mathematical view of automatic differentiation. *Acta Numerica*, 12:321–398, 2003.
- [22] Diederik P Kingma and Jimmy Ba. Adam: A method for stochastic optimization. *arXiv preprint arXiv:1412.6980*, 2014.

- [23] Patrick Koch, Oleg Golovidov, Steven Gardner, Brett Wujek, Joshua Griffin, and Yan Xu. Autotune: A derivative-free optimization framework for hyperparameter tuning. In *Proceedings of the 24th ACM SIGKDD international conference on knowledge discovery & data mining*, pages 443–452, 2018.
- [24] Lingkai Kong, Yuqing Wang, and Molei Tao. Momentum stiefel optimizer, with applications to suitably-orthogonal attention, and optimal transport. *arXiv preprint arXiv:2205.14173*, 2022. Published as a conference paper at ICLR 2023.
- [25] Frederik Kunstner, Philipp Hennig, and Lukas Balles. Limitations of the empirical fisher approximation for natural gradient descent. *Advances in neural information processing systems*, 32, 2019.
- [26] Serge Lang. *Fundamentals of differential geometry*, volume 191. Springer Science & Business Media, 2012.
- [27] Mario Lezcano-Casado and David Martinez-Rubio. Cheap orthogonal constraints in neural networks: A simple parametrization of the orthogonal and unitary group. In *International Conference on Machine Learning*, pages 3794–3803. PMLR, 2019.
- [28] Jun Li, Li Fuxin, and Sinisa Todorovic. Efficient riemannian optimization on the stiefel manifold via the cayley transform. *arXiv preprint arXiv:2002.01113*, 2020. Published as a conference paper at ICLR 2020.
- [29] Wu Lin, Valentin Duruisseaux, Melvin Leok, Frank Nielsen, Mohammad Emtiyaz Khan, and Mark Schmidt. Simplifying momentum-based riemannian submanifold optimization. *arXiv preprint arXiv:2302.09738*, 2023.
- [30] Francesco Mezzadri. How to generate random matrices from the classical compact groups. *arXiv preprint math-ph/0609050*, 2006.
- [31] Barrett O’neill. *Semi-Riemannian geometry with applications to relativity*. Academic press, New York City, New York, 1983.
- [32] Maziar Raissi, Paris Perdikaris, and George E Karniadakis. Physics-informed neural networks: A deep learning framework for solving forward and inverse problems involving nonlinear partial differential equations. *Journal of Computational physics*, 378:686–707, 2019.
- [33] Wolfgang Ring and Benedikt Wirth. Optimization methods on riemannian manifolds and their application to shape space. *SIAM Journal on Optimization*, 22(2):596–627, 2012.
- [34] Ahmed Salam, Anas El Farouk, and Eman Al-Aidarous. Symplectic householder transformations for a qr-like decomposition, a geometric and algebraic approaches. *Journal of computational and applied mathematics*, 214(2):533–548, 2008.
- [35] Hiroyuki Sato. *Riemannian optimization and its applications*, volume 670. Springer-Verlag, Heidelberg, Germany, 2021.
- [36] Markus Schlarb. Covariant derivatives on homogeneous spaces: Horizontal lifts and parallel transport. *The Journal of Geometric Analysis*, 34(5):1–43, 2024.

- [37] Jorge Nocedal Stephen J. Wright. *Numerical optimization*. Springer Science+Business Media, New York, NY, 2006.
- [38] Nicky J van den Berg, Bart MN Smets, Gautam Pai, Jean-Marie Mirebeau, and Remco Duits. Geodesic tracking via new data-driven connections of cartan type for vascular tree tracking. *Journal of Mathematical Imaging and Vision*, 66(2):198–230, 2024.
- [39] Ashish Vaswani, Noam Shazeer, Niki Parmar, Jakob Uszkoreit, Llion Jones, Aidan N Gomez, Łukasz Kaiser, and Illia Polosukhin. Attention is all you need. *Advances in neural information processing systems*, 30, 2017.
- [40] Han Xiao, Kashif Rasul, and Roland Vollgraf. Fashion-mnist: a novel image dataset for benchmarking machine learning algorithms. *arXiv preprint arXiv:1708.07747*, 2017.
- [41] Aston Zhang, Alvin Chan, Yi Tay, Jie Fu, Shuohang Wang, Shuai Zhang, Hua-jie Shao, Shuochao Yao, and Roy Ka-Wei Lee. On orthogonality constraints for transformers. In *Proceedings of the 59th Annual Meeting of the Association for Computational Linguistics and the 11th International Joint Conference on Natural Language Processing*, volume 2, pages 375–382. Association for Computational Linguistics, 2021.

A Induced Isomorphism

The mapping Ω in equation Equation (14) can be easily shown to established the isomorphism $T_Y\mathcal{M} \xrightarrow{\sim} \mathfrak{g}^{\text{hor},Y}$:

$$\begin{aligned} \Omega(\text{rgrad}(Y, \nabla L))Y &= \left(I - \frac{1}{2}YY^T\right)\text{rgrad}(Y, \nabla L) - \frac{1}{2}Y(\text{rgrad}(Y, \nabla L))^TY = \\ &= \left(I - \frac{1}{2}YY^T\right)\text{rgrad}(Y, \nabla L) + \frac{1}{2}YY^T\text{rgrad}(Y, \nabla L) = \text{rgrad}(Y, \nabla L), \end{aligned} \quad (23)$$

where it was used that $\text{grad}(Y, \nabla L) \in T_Y\mathcal{M}$, i.e. $(\text{grad}(Y, \nabla L))^TY = Y^T\text{grad}(Y, \nabla L)$.

B Computing the Lift $Y \mapsto \lambda(Y)$

Algorithm 2 uses a QR decomposition, or more precisely, Householder reflections. These are implemented in most numerical linear algebra libraries.

In essence, Householder reflections take as input an $N \times M$ matrix and transform it to an upper-triangular one by a series of M rotations. These rotations are stored in the Q matrix of the QR decomposition.¹⁵

The computation of the section Λ is shown in Algorithm 2. The following is needed to ensure λ is in fact a lift to $G = O(N)$:

Proposition 2. *Let $Y \in \mathbb{R}^{N \times n}$ be a matrix whose columns are orthonormal, $A \in \mathbb{R}^{N \times (N-n)}$ be such that $Y^TA = \mathbb{O}_n$ and $QR = A$ its decomposition. Then $Q^TY = \mathbb{O}_n$.*

Proof. Write $Q = [q_1, \dots, q_{N-n}, \dots]$. The special structure of R (i.e. $[R]_{ij} =: r_{ij} = 0$ for $i > j$) means that the first column of $A =: [a_1, \dots, a_{N-n}]$ is a linear combination of $\{q_1\}$, the second column is a linear combination of $\{q_1, q_2\}$ and so forth. But this in turn means that every q_i ($i = 1, \dots, (N-n)$) can be constructed with columns of A . Thus Q and A span the same vector space, and this vector space is orthogonal to Y by assumption. \square

It should be noted that this specific part of the algorithm is also extendable to, for example, the symplectic Stiefel manifold, as there also exists a Householder routine for this [34]. Other QR decompositions may also be used for this step.

C Computing Exponentials

As was already discussed by other authors [5, 18, 16, 12], computing the matrix exponential to solve the geodesic in Theorem 2 for a matrix manifold with large dimension N and small dimension n only requires computing a matrix exponential of a $2n \times 2n$ dimensional matrix.

The implementation of our algorithm uses the following (also see [12, proposition 3] and [5, proposition 3.8]): The elements of $\mathfrak{g}^{\text{hor}}$ have a special block structure (see equation Equation (16)) that allows each matrix to be written in the following form:

$$\mathfrak{g}^{\text{hor}} = \left\{ \begin{bmatrix} \frac{1}{2}A & \mathbb{I}_n \\ B & \mathbb{O} \end{bmatrix} \begin{bmatrix} \mathbb{I}_n & \mathbb{O}^T \\ \frac{1}{2}A & -B^T \end{bmatrix} : A \in \mathbb{R}^{n \times n} \text{ skew-sym}, B \in \mathbb{R}^{N \times n} \text{ arbitrary} \right\}. \quad (24)$$

¹⁵ R is the upper-triangular matrix resulting from the transformations. A detailed description of Householder reflections is given in e.g. [30].

The computation of the geodesic can be performed cheaply by recognizing the following (the two block matrices in equation Equation (24) will be called B' and B''^T with $B', B'' \in \mathbb{R}^{N \times 2n}$):

$$\exp(B' B''^T) = \sum_{n=0}^{\infty} \frac{1}{n!} (B' B''^T)^n = \mathbb{I}_N + \sum_{n=1}^{\infty} \frac{1}{n!} B' (B''^T B')^{n-1} B''^T \quad (25)$$

$$= \mathbb{I}_N + B' \left(\sum_{n=1}^{\infty} \frac{1}{n!} (B''^T B')^{n-1} \right) B''. \quad (26)$$

The expression $\mathfrak{A}(B', B'') := \sum_{n=1}^{\infty} \frac{1}{n!} (B''^T B')^{n-1}$ only involves matrix products of $2n \times 2n$ matrices and can be solved cheaply. To do so we rely on a simple Taylor series expansion:

Algorithm 4 Evaluation of the quantity $\mathfrak{A}(B', B'') \equiv \mathfrak{A}(B''^T B')$.

```

output  $\leftarrow$   $\mathbb{I}$ , product  $\leftarrow$   $\mathbb{I}$ ,  $t \leftarrow 1$ ,
while ||product|| <  $\varepsilon$  do
     $t \leftarrow t + 1$ ,
    product  $\leftarrow$   $\frac{1}{t}$  product *  $(B''^T B')$ ,
    output  $\leftarrow$  output + product
end while

```

Here ε denotes machine precision. With this the retraction takes the form:

$$\begin{aligned} \mathcal{R}_Y^{\text{geo}}(\Delta) &\equiv \lambda(Y) \text{retraction}(B) \\ &= Y + \lambda(Y) \begin{bmatrix} \frac{1}{2}A & \mathbb{I}_n \\ B & \mathbb{O} \end{bmatrix} \mathfrak{A} \left(\begin{bmatrix} \frac{1}{2}A & \mathbb{I}_n \\ \frac{1}{4}A^2 - B^T B & \frac{1}{2}A \end{bmatrix} \right) \begin{bmatrix} \mathbb{I}_n \\ \frac{1}{2}A \end{bmatrix}, \end{aligned} \quad (27)$$

where the matrix exponential is now only computed for a *small* $2n \times 2n$ matrix.

D The Cayley Retraction

Perhaps the most common example for matrix manifolds is the *Cayley retraction*. It is a retraction for many matrix Lie groups [1, 5]. For $V \in T_{\mathbb{I}}G \equiv \mathfrak{g} = \mathfrak{so}(N)$ it is defined as

$$\text{Cayley}(V) = \left(\mathbb{I} - \frac{1}{2}V \right)^{-1} \left(\mathbb{I} + \frac{1}{2}V \right). \quad (28)$$

We can also use the Cayley retraction at a different point than the identity \mathbb{I} . For this consider $\bar{A} \in O(N)$ and $\bar{B} \in T_{\bar{A}}O(N) = \{\bar{B} \in \mathbb{R}^{N \times N} : \bar{A}^T \bar{B} + \bar{B}^T \bar{A} = \mathbb{O}\}$. We then have $\bar{A}^T \bar{B} \in \mathfrak{so}(N)$ and

$$\overline{\text{Cayley}} : T_{\bar{A}}O(N) \rightarrow O(N), \bar{B} \mapsto \bar{A} \text{Cayley}(\bar{A}^T \bar{B}), \quad (29)$$

is a retraction $\forall \bar{A} \in O(N)$.

Similar to the *geodesic retraction* (see Appendix C) we also leverage the decomposition of $\bar{B} = B'(B'')^T \in \mathfrak{g}^{\text{hor}}$ for the Cayley retraction. Here we do this through the *Sherman-Morrison-Woodbury formula* [37]:

$$(\mathbb{I}_N - \frac{1}{2}B'(B'')^T)^{-1} = \mathbb{I}_N + \frac{1}{2}B'(\mathbb{I}_{2n} - \frac{1}{2}B'(B'')^T)^{-1}(B'')^T \quad (30)$$

So what we have to compute the inverse of:

$$\mathbb{I}_{2n} - \frac{1}{2} \begin{bmatrix} \mathbb{I} & \mathbb{O}^T \\ \frac{1}{2}A & -B^T \end{bmatrix} \begin{bmatrix} \frac{1}{2}A & \mathbb{I}_n \\ B & \mathbb{O} \end{bmatrix} = \begin{bmatrix} \mathbb{I}_n - \frac{1}{4}A & -\frac{1}{2}\mathbb{I}_n \\ \frac{1}{2}B^T B - \frac{1}{8}A^2 & \mathbb{I}_n - \frac{1}{4}A \end{bmatrix}, \quad (31)$$

where A and B describe an element of $\mathfrak{g}^{\text{hor}}$ (see Equation (16)). By leveraging the sparse structure of the matrices in $\mathfrak{g}^{\text{hor}}$ we arrive at the following expression for the Cayley retraction (similar to the case of the geodesic retraction):

$$\text{Cayley}(\bar{B}) = \mathbb{I}_N + \frac{1}{2}B' \left(\mathbb{I}_{2n} - \frac{1}{2}(B'')^T B' \right)^{-1} (B'')^T \left(\mathbb{I}_N + \frac{1}{2}\bar{B} \right). \quad (32)$$

Similar to the geodesic retraction, here the expensive operation (the matrix inverse in this case) is only computed for a small $2n \times 2n$ matrix.

E Parallel Transport

Here we show that our algorithm *parallel transports* the cache along the curve defined by the retraction.

The concept of *parallel transport along a geodesic* $\gamma : [0, T] \rightarrow \mathcal{M}$ describes moving a tangent vector from $T_x\mathcal{M}$ to $T_{\gamma(t)}\mathcal{M}$ such that its orientation with respect to the geodesic is preserved.

A precise definition of parallel transport needs a notion of a *connection* [26, 8, 6] and we forego it here. We simply state how to parallel transport vectors on the Lie group $O(N)$ and the homogeneous space $St(n, N)$.

Proposition 3. *Given two elements $B_1^A, B_2^A \in T_A G$ the parallel transport of B_2^A along the geodesic of B_1^A is given by*

$$\Pi_{A \rightarrow \gamma_{B_1^A}(t)} B_2^A = A \exp(t \cdot A^{-1} B_1^A) A^{-1} B_2^A = A \exp(t \cdot B_1) B_2, \quad (33)$$

where $B_i := A^{-1} B_i^A$.

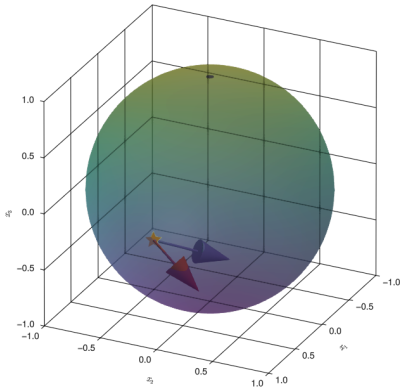
For the Stiefel manifold this is not much more complicated¹⁶:

Proposition 4. *Given two elements $\Delta_1, \Delta_2 \in T_Y \mathcal{M}$, the parallel transport of Δ_2 along the geodesic of Δ_1 is given by*

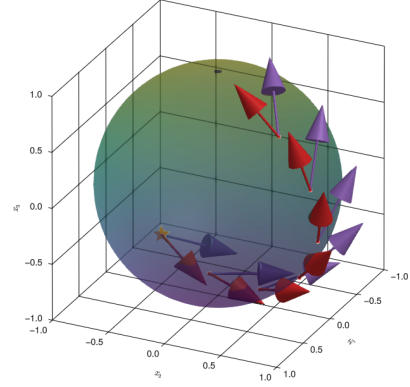
$$\Pi_{Y \rightarrow \gamma_{\Delta_1}(t)} \Delta_2 = \exp(t \cdot \Omega(\Delta_1)) \Delta_2 = \lambda(Y) \exp(\mathcal{B}_1) \lambda(Y)^{-1} \Delta_2, \quad (34)$$

where $\mathcal{B}_1 = \lambda(Y)^{-1} \Omega(\Delta_1) \lambda(Y)$.

¹⁶Here we do not provide a detailed proof that this constitutes a sound expression from the perspective of Riemannian geometry. A proof can be found in [36].



(a) The red vector v_1 represents the *final velocity* and the purple vector v_2 represents the *cache* of the optimizer.



(b) Here the geodesic equation has been solved for v_1 for different time steps η and v_2 has been parallel-transported along it.

Figure 7: Visualization of parallel transport.

We can further modify the expression of parallel transport for the Stiefel manifold:

$$\Pi_{Y \rightarrow \gamma_{\Delta_1}(t)} \Delta_2 = \lambda(Y) \exp(\mathcal{B}_1) \lambda(Y) \Omega(\Delta_2) Y = \lambda(Y) \exp(\mathcal{B}_1) \mathcal{B}_2 E, \quad (35)$$

where $\mathcal{B}_2 = \lambda(Y)^{-1} \Omega(\Delta_2) \lambda(Y)$. We can now define explicit updating rules for the global section $\Lambda^{(\cdot)}$ (this is the operation `update_section` in Algorithm 1), the element of the homogeneous space $Y^{(\cdot)}$, the tangent vector $\Delta^{(\cdot)}$ and $D^{(\cdot)} = (\Lambda^{(\cdot)})^{-1} \Omega(\Delta^{(\cdot)}) \Lambda^{(\cdot)}$, its representation in $\mathfrak{g}^{\text{hor}}$.

We thus have:

1. $\Lambda^{(t+1)} \leftarrow \Lambda^{(t)} \exp(\mathcal{B}^{(t)}) = \text{update_section}(\Lambda^{(t)}, \mathcal{B}^{(t)})$,
2. $Y^{(t+1)} \leftarrow \Lambda^{(t+1)} E$,
3. $\Delta^{(t+1)} \leftarrow \Lambda^{(t)} \exp(\mathcal{B}^{(t-1)}) (\Lambda^{(t)})^{-1} \Delta^{(t)} = \Lambda^{(t+1)} D^{(t)} E$,
4. $D^{(t+1)} \leftarrow D^{(t)}$.

So we conveniently take parallel transport of vectors into account by representing them in $\mathfrak{g}^{\text{hor}}$: D does not change, i.e. we always have $D^{(t+1)} = D^{(t)}$.

To demonstrate parallel transport we compute the geodesic along a vector and parallel transport another one along this geodesic. The result is shown in Appendix E.

Here we perform parallel transport on the homogeneous space $S^2 = St(1, 3)$, i.e. the sphere. Figure 7(a) shows the two vectors before the geodesic is solved. We then compute $\text{geodesic}(\eta \cdot v_1)$, where v_1 is the red vector, for a number of steps η . The purple vector, which we call v_2 , is parallel transported along the geodesic determined by v_1 . When training a neural network v_1 can be seen as *final velocity*, i.e. the output of an optimizer method (confer Algorithm 1 and definition 1), and v_2 can be seen as the *cache* belonging to that optimizer.

F The Softmax Activation Function and the Classification Layer

The softmax function maps an arbitrary vector $v \in \mathbb{R}^\ell$ to a probability vector $\text{softmax}(v) \in \{w \in (0, 1)^\ell : \sum_{i=1}^\ell w_i = 1\}$ via

$$\text{softmax}(v) = \frac{\exp(v_i)}{\sum_{i=1}^\ell \exp(v_i)}. \quad (36)$$

In Section 4 we referred to a prediction of the form $(0, \dots, 1, \dots, 0) =: e_i$, i.e. a vector that has entry 1 at the i -th slot and zeros at all others, as a *trivial prediction*. This is what is learned by the network in Figure 5 if we do not constrain the projection matrices to be on the Stiefel manifold. The loss in Figure 6 for the case of unconstrained weights (blue lines) is consistently stuck at around 1.34; this is because the output of the network is always e_i and the target is a vector $t \in \{0, 1\}^{10}$ with zeros everywhere except for one component. So the resulting L_2 error is

$$\sqrt{\frac{9}{10}} \cdot 2 \approx 1.34, \quad (37)$$

which is what we see in Figure 6.

G Computing Correlations in the Multihead-Attention Layer

In Section 4 multihead attention was described in three steps. Here we elaborate on the second one of these and argue why it makes sense to constrain the projection matrices to be part of the Stiefel manifold.

The *attention mechanism* in equation Equation (20) describes a reweighting of the “values” V_i based on correlations between the “keys” K_i and the “queries” Q_i . First note the structure of these matrices: they are all a collection of 16 7-dimensional vectors, i.e. $V_i = [v_i^{(1)}, \dots, v_i^{(16)}]$, $K_i = [k_i^{(1)}, \dots, k_i^{(16)}]$ and $Q_i = [q_i^{(1)}, \dots, q_i^{(16)}]$. Those vectors have been obtained by applying the respective projection matrices onto the original image $I_i \in \mathbb{R}^{49 \times 16}$.

When performing the *reweighting* of the columns of V_i we first compute the correlations between the vectors in K_i and in Q_i and store the results in a *correlation matrix* C_i :

$$[C_i]_{mn} = \left(k_i^{(m)}\right)^T q_i^{(n)}. \quad (38)$$

The columns of this correlation matrix are then rescaled with a softmax function, obtaining a matrix of *probability vectors* \mathcal{P}_i :

$$[\mathcal{P}_i]_{\bullet n} = \text{softmax}([C_i]_{\bullet n}). \quad (39)$$

Finally the matrix \mathcal{P}_i is multiplied onto V_i from the right, resulting in 16 convex combinations of the 16 vectors $v_i^{(m)}$ with $m = 1, \dots, 16$:

$$V_i \mathcal{P}_i = \left[\sum_{m=1}^{16} [\mathcal{P}_i]_{m1} v_i^{(m)}, \dots, \sum_{m=1}^{16} [\mathcal{P}_i]_{m16} v_i^{(m)} \right]. \quad (40)$$

With this we can now give a better interpretation of what the projection matrices W_i^V , W_i^K and W_i^Q should do: they map the original data to lower-dimensional subspaces. We then compute correlations between the representation in the K and in the Q basis and use this correlation to perform a convex reweighting of the vectors in the V basis. These reweighted *values* are then fed into a standard feedforward neural network.

Because the main task of the W_i^V , W_i^K and W_i^Q matrices here is for them to find bases, it makes sense to constrain them onto the Stiefel manifold; they do not need to have the maximum possible generality.